

# Charm particle production in hadronic collisions

C. Avila<sup>1)\*</sup>, J. Magnin<sup>1,2)†</sup>, L.M. Mendoza-Navas<sup>1)‡</sup>

<sup>1)</sup> *Departamento de Física, Universidad de los Andes*

A.A. 4976, Santafé de Bogotá, Colombia

<sup>2)</sup> *Centro Brasileiro de Pesquisas Físicas*

Rua Dr. Xavier Sigaud 150, Urca, CEP 22290-180, Rio de Janeiro, Brazil

February 1, 2008

## Abstract

We study charm particle production in hadron-hadron collisions. After calculating perturbatively the charm quark differential cross section, we study the hadronization mechanisms. It is shown that recombination is the key to understand the so called Leading Particle Effect in charm meson production. For charm baryon production, however, leading particle effects are due to a combination of contributions coming from both, the recombination and the fragmentation mechanisms. We compare our calculations to experimental data on charm hadron production in  $\pi^- N$  and  $p N$  interactions from several experiments and show that a consistent description of them can be reached without the aid of other mechanism than recombination and fragmentation.

---

\*cavila@uniandes.edu.co

†jmagnin@cbpf.br

‡luismi@fnal.gov

# 1 Introduction

Heavy quark production in hadronic collisions is one of the most interesting testing grounds of Quantum Chromodynamics. The fusion reactions  $g g \rightarrow Q \bar{Q}$  and  $q \bar{q} \rightarrow Q \bar{Q}$  are expected to be dominant in heavy quark,  $Q$ , production and, as a matter of fact experimental data seems to reasonably agree with perturbative QCD (pQCD) calculations which today are available up to Next to Leading Order (NLO) [1].

Once a heavy quark is produced, it has to hadronize to produce the observed, hadronic, final state. On this respect, it was expected that the factorization theorem be valid and hadronization proceeded through the fragmentation mechanism. Thus, heavy hadron production can be separated into the perturbatively calculable hard scattering and gluon dynamics from the non-perturbative bound state dynamics contained in the process independent hadron structure, expressed through the corresponding parton distribution functions (PDF),  $q(x, Q^2)$  and  $g(x, Q^2)$ , and the jet fragmentation functions,  $D_{h/Q}(z, Q^2)$ <sup>1</sup>. Literally speaking, the factorization assumption predicts strict independence of the heavy quark hadronization from the production process. Thus, no flavor correlation should exist between initial and final states.

However, there exist copious experimental information on charm hadron production which contradicts the above hypothesis [2, 3, 4, 5, 6, 7, 8, 9]. In fact, there was observed an excess in the charm hadron production at large values of  $x_F$  ( $\sim 2p_l/\sqrt{s}$ ) and a correlation between the leading<sup>2</sup> charm hadrons with the projectile quantum numbers. This suggests the presence of other hadronization mechanisms which must be relevant at large values of  $x_F$  and low  $p_T^2$ , as long as fragmentation of the charm quark should not produce either flavor correlations between initial and final states, neither charm hadrons at large values of  $x_F$ . In particular, flavor correlation suggests hadronization mechanisms by which projectile spectators produced at small  $p_T^2$  recombine with charm quarks produced either perturbatively in the hard QCD process, or charm quarks, though perhaps of a non-perturbative nature, already present in the structure of the beam particles.

From a theoretical point of view, models have been proposed to account for the enhancement of charm hadron production at large  $x_F$  and flavor correlations. Among them we can mention the model of Ref [10], in which a charm quark produced perturbatively recombines with the debris of the projectile, the intrinsic charm model [11], in which a particular Fock state of the projectile containing charm quarks breaks in the collision giving thus the desired flavor correlation between initial and final particles, recombination type models [12] in which charm quarks already present in the projectile structure recombine with light quarks, and models based in the Dual Parton Model and Dual Topological Unitarization [13] in which both, the heavy quark

---

<sup>1</sup> $x$  is the momentum fraction of partons inside the initial hadron,  $z$  is the momentum fraction of the heavy quark in the final hadron.  $Q^2$  is the momentum transfer.

<sup>2</sup>A leading particle is defined as the one which shares valence quarks with the colliding hadrons

production and hadronization, are treated on a non-perturbative basis. Likewise, most recently two new approaches based in recombination have been presented. In the first, recombination of charm and light quarks, both being part of a hard QCD diagram, recombine to produce a charm hadron [14]. In this scheme, recombination is thought as a higher order correction to hadronization since hard scattering diagrams contributing to this process are of NLO or higher. The second approach [15] involves a modification of the usual recombination prescription to produce an enhancement in the central (low  $x_F$ ) production of charm hadrons.

All the above models have been more or less successful in reproducing the main features of charm hadron production, with possibly the only exception of the intrinsic charm model [11], which seems to be excluded [16] by recent experimental data on charm baryon production in  $\pi^- N$  interactions by the E791 [2] and SELEX [3] Collaborations. However, it is important to remark that, although some models are able to reproduce experimental data on production asymmetries, they cannot reproduce simultaneously data on production asymmetries and differential cross sections. This is the case of the intrinsic charm model, as noted in Ref. [16]. This shows that in order to make a meaningful comparison among models and experimental data, both, the differential cross section and the production asymmetry have to be taken properly into account. As a matter of fact, we have two out of three quantities which are independent, namely, the differential cross sections of both, particle and antiparticle, or one of the cross sections and the production asymmetry.

In what follows we shall analyse the main features of perturbative charm production in hadron-hadron collisions followed by the study of possible hadronization mechanisms. Later, we will compare model results with available experimental data. The last section will be devoted to conclusions.

## 2 Brief review of perturbative charm production

In the parton model, charm quarks are produced through the interaction of partons in the initial hadrons. The differential cross section as a function of  $x_F$  is given by [17]

$$\frac{d\sigma_{c(\bar{c})}}{dx_F} = \frac{1}{2}\sqrt{s} \int H_{ab}(x_a, x_b, \mu_F^2, \mu_R^2) \frac{1}{E} dp_T^2 dy, \quad (1)$$

where  $H_{ab}$  is a function containing information on the structure of the colliding hadrons  $a, b$ , and on the hard QCD process which produces the charm quarks. At LO, the function  $H_{ab}$  reads

$$\begin{aligned} H_{ab}(x_a, x_b, \mu_F^2, \mu_R^2) = & \Sigma_i \left( q_i^a(x_a, \mu_F^2) \bar{q}_i^b(x_b, \mu_F^2) \right. \\ & + \bar{q}_i^a(x_a, \mu_F^2) q_i^b(x_b, \mu_F^2) \Big) \frac{d\hat{\sigma}}{d\hat{t}} \Big|_{q\bar{q}}(\hat{s}, m_c, \mu_R^2) \\ & + g_i^a(x_a, \mu_F^2) g_i^b(x_b, \mu_F^2) \frac{d\hat{\sigma}}{d\hat{t}} \Big|_{gg}(\hat{s}, m_c, \mu_R^2), \end{aligned} \quad (2)$$

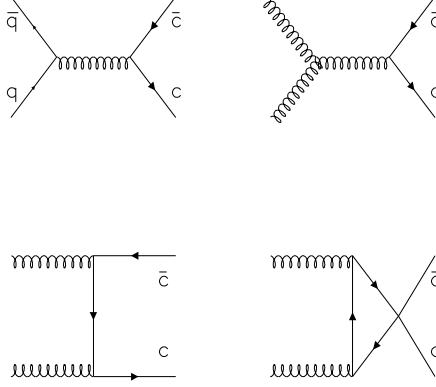


Figure 1: Feynman diagrams for the elementary cross sections entering in eqs. (3) and (4) at LO.

with  $x_a$  and  $x_b$  being the parton momentum fractions,  $q(x, \mu_F^2)$  and  $g(x, \mu_F^2)$  the quark and gluon momentum distributions in the colliding particles,  $\hat{s} = x_a x_b s$  is the square of c.m. energy of the partonic system and  $\mu_F$  and  $\mu_R$  are the factorization and the renormalization scales respectively. In eq. (1),  $p_T^2$  is the squared transverse momentum of the produced  $c$ -quark,  $y$  is the rapidity of the  $\bar{c}$  quark and  $E$  the energy of the produced  $c$ -quark. The sum in eq. (2) runs over  $i = u, \bar{u}, d, \bar{d}, s, \bar{s}$ .

The elementary cross-sections for  $q - \bar{q}$  annihilation and gluon fusion,  $d\hat{\sigma}/d\hat{t}|_{q\bar{q}}$  and  $d\hat{\sigma}/d\hat{t}|_{gg}$  respectively, at LO are given by [17, 18].

$$\frac{d\hat{\sigma}}{d\hat{t}}|_{q\bar{q}} = \frac{\pi\alpha_s^2(\mu_R^2)}{9\hat{m}_c^4} \frac{\cosh(\Delta y) + m_c^2/\hat{m}_c^2}{[1 + \cosh(\Delta y)]^3} \quad (3)$$

$$\frac{d\hat{\sigma}}{d\hat{t}}|_{gg} = \frac{\pi\alpha_s^2(\mu_R^2)}{96\hat{m}_c^4} \frac{8\cosh(\Delta y) - 1}{[1 + \cosh(\Delta y)]^3} \left[ \cosh(\Delta y) + \frac{2m_c^2}{\hat{m}_c^2} + \frac{2m_c^4}{\hat{m}_c^4} \right], \quad (4)$$

where  $\Delta y$  is the rapidity gap between the produced  $c$  and  $\bar{c}$  quarks and  $\hat{m}_c^2 = m_c^2 + p_T^2$ . The Feynman diagrams involved in the calculation of eqs. (3) and (4) are shown in Fig. 1.

As shown in eqs. (3-4), at LO the only dependence on  $\mu_R$  in the elementary cross sections is in  $\alpha_s^2(\mu_R^2)$ . At this order, the value of the renormalization scale is fixed by the requirement that the propagators in diagrams of Fig. 1 be off-shell by a quantity of at least  $m_c^2$ . So, it is common to use  $\mu_R^2 = m_c^2$ .

Concerning the factorization scale  $\mu_F$ , it is the scale at which the initial hadrons “see” one another in the collision. Then, in the above sense,  $\mu_F$  gives the quark and gluon content of the initial hadrons at the time of the collision. However, differently to the case of the renormalization scale  $\mu_R$ , there is no guiding principle to help fixing  $\mu_F$ . Along this work, and in order to avoid problems related with flavor excitation diagrams containing heavy quarks [1, 18], we shall use  $\mu_F = 1$  GeV, below the threshold for charm production and consistent with the sum over light flavors in eq. (2).

It is also known that NLO and LO calculations only differ by a  $K$ -factor of the order of  $2 - 3$  [19], meaning that calculations can be done consistently at LO and then multiplied by the corresponding  $K$ -factor. NLO calculations also show a tiny  $c - \bar{c}$  asymmetry [1], which is too small to produce any effect after hadronization. Note however that, although the small  $c - \bar{c}$  asymmetry arising at NLO has the same sign that the observed  $D^+ - D^-$  production asymmetry (i.e.  $\bar{c}$  and  $D^-$  favored over  $c$  and  $D^+$  production), it has the opposite sign for baryon production.

### 3 Hadronization mechanisms

There are basically two different models for charm quark hadronization, namely, recombination and fragmentation. In the first, the  $c$  ( $\bar{c}$ )-quark produced in a pQCD process joins to the debris of the initial particles to form the final charm hadron [10] while in the second, the  $c$  ( $\bar{c}$ )-quark fragments to the final charm hadron leaving a string of quarks behind it [20]. Variation of these processes can also be found in the literature [21]. However, there are some features which are common to any class of hadronization processes: hadrons are colorless, which means that hadronizing quarks must be in a color singlet state and, at the end of hadronization, no free quarks could exist any more. These two basic requirements are the consequence of confinement in QCD. Consequently, whatever the hadronization process be, a color string must be formed among the hadronizing quarks which has to have the correct color quantum numbers and the exact number of quarks to ensure that no free quarks remain at the end of the process and colorless hadrons are formed. These lead us to the following classification: *i) Short color strings*, responsible for recombination processes, in which a  $q - \bar{q}$  pair or a  $qqq$  forms the final hadron without further hadron emission, and *ii) Large color strings*, producing the final hadron by fragmentation being it accompanied by the emission of light (mostly pion) mesons. Note that, in addition, for each case there exist also two different types of color strings, namely, the meson and the baryon-like strings, being them characterized by the fact that the first is formed among a quark and an antiquark and the second one between a quark and a diquark, as shown in Fig. 2. The first will produce predominantly mesons while the later has to produce at least one baryon in order to conserve the baryon number.

In what follows, we will analyze both, fragmentation and recombination, having

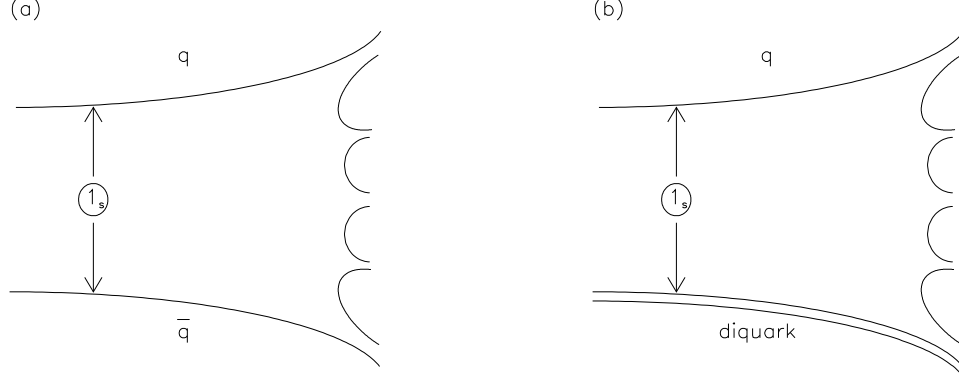


Figure 2: Allowed color string configurations: meson-like string (a) and baryon-like string (b).

in mind their applicability to heavy quark hadronization process.

### 3.1 Fragmentation

A typical quark configuration leading to fragmentation is shown in Fig. 3. Formation of color strings among the charm quarks and the remnants of the colliding hadrons would give rise to the production of open charm, i.e.  $D$  mesons and eventually charm baryons.

This kind of contribution to hadronization is usually modeled by the convolution of the  $c$ -quark differential cross section with a Peterson Fragmentation Function,  $D_{H/c}$ , [20],

$$\begin{aligned} \frac{d\sigma_H}{dx_F} &= \int \frac{dz}{z} \frac{d\sigma_{c(\bar{c})}}{dx} D_{H/c}(z) , \\ z &= \frac{x_F}{x} , \\ D_{H/c}(z) &= \frac{N}{z \left(1 - \frac{1}{z} - \frac{\epsilon}{1-z}\right)^2} , \end{aligned} \tag{5}$$

where  $d\sigma_{c(\bar{c})}/dx$  is given in eq. (1). Along this work we will use  $\epsilon = 0.022$  for  $D$  meson production and  $\epsilon = 0.06$  for  $\Lambda_c$ . These values for  $\epsilon$  have been extracted from charm hadron production in  $e^+ - e^-$  interactions [22]. Note that the fragmentation function

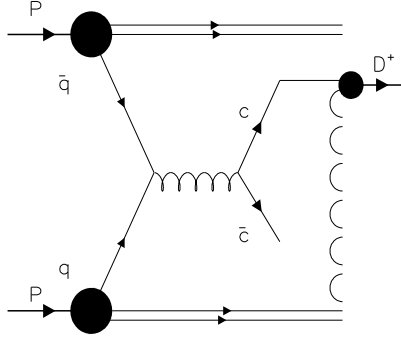


Figure 3: Typical configuration leading to  $D^+$  production in  $p - p$  interactions by color string fragmentation.

is used to model the production of a hadron containing a heavy quark at the end of the color string, regardless of what happens with the remaining of the color string.

### 3.2 Recombination

A typical quark configuration leading to recombination is shown in Fig. 4. The contribution of the recombination mechanism can be estimated by means of [10]

$$\frac{d\sigma}{dx_F} = \frac{\sqrt{s}}{2} \int x_v z^* \frac{d\sigma^*}{dx_v dz} R(x_v, z, x_F) \frac{dx_v}{x_v} \frac{dz}{z} , \quad (6)$$

where  $R(x_v, z, x_F)$  is the recombination function, for which we shall use [24]

$$R(x_v, z, x_F) = \beta \frac{x_v z}{x_F^2} \delta \left( 1 - \frac{x_v + z}{x_F} \right) , \quad (7)$$

with  $\beta$  a normalization parameter which has to be fixed from experimental data. In eq. (6),  $z^* = 2E_c/\sqrt{s}$  and

$$\begin{aligned} \frac{d\sigma^*}{dx_v dz} &= q_v(x_v, \mu_F^2) \frac{d\hat{\sigma}}{dx_v dz} , \\ \frac{d\hat{\sigma}}{dx_v dz} &= \int_0^W dp_T^2 \int_{z_+/(1-z_-)}^{1-x_v} \frac{H_{ab}(x_a, x_b, \mu_F^2, \mu_R^2)}{x_a - z_+} dx_a , \end{aligned} \quad (8)$$

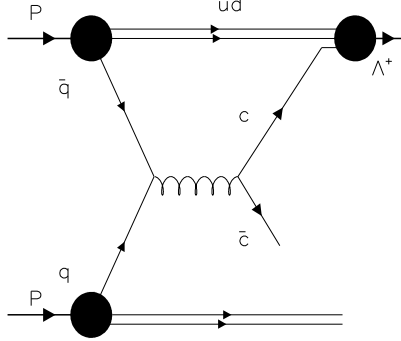


Figure 4: Typical configuration leading to  $\Lambda_c^+$  production in  $p - p$  interactions by recombination.

where  $H_{ab}$  is given in eq. (2),  $x_v$  is the fraction of the momentum of the hadron  $a$  carried by the spectator quark  $q_v$ ,  $z = 2p_{z,c}/\sqrt{s}$ ,  $z_{\pm} = \frac{1}{2}(z^* \pm z)$ ,  $x_b = x_a z_- / (x_a - z_+)$  and

$$\begin{aligned} E_c &= \sqrt{m_T^2 + p_{z,c}^2}, \\ W &= \frac{s(1 - x_v - z)(1 - x_v)(1 + z)}{(2 - x_v)^2} - m_c^2. \end{aligned} \quad (9)$$

In eq. (8),  $q_v$  is the probability density function of a quark in the initial hadron. For baryon production,  $q_v$  has to be replaced by  $q_v(x_{v1}, x_{v2}, \mu_F^2) = q_{v1}(x_{v1}, \mu_F^2) q_{v2}(x_{v2}, \mu_F^2)$  and the recombination function of eq. (7) by [25]

$$R(x, y, z, x_F) = \beta \frac{x y z}{x_F^3} \delta\left(1 - \frac{x + y + z}{x_F}\right). \quad (10)$$

Notice that, as the quark  $q_v$  contains information about the structure of one of the colliding hadrons, this introduces a flavor correlation among the initial and final states.

### 3.3 Direct recombination

A second possibility is that a *spectator* charm quark in a flavor excitation subdiagram recombines with the debris of one of the initial hadrons as shown in Fig. 5. This



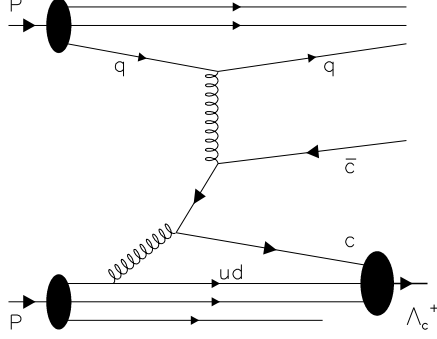


Figure 5: Typical configuration leading to  $\Lambda_c^+$  production in  $p - p$  interactions by spectator recombination.

kind of contributions can be calculated along the lines of the model of Refs. [12, 23] in which a charm quark being part of the sea of the initial hadron recombines with valence and sea quarks after the collision. Notice, however, that the factorization scale must be consistent with the fact that charm quarks exist in the sea of the initial hadron, i.e.  $\mu_F^2 \geq m_c^2$ . The production of charm mesons is then given by [24]

$$\frac{d\sigma^{rec}}{dx_F} = \beta \int_0^{x_F} \frac{dx_1}{x_1} \frac{dx_2}{x_2} F_2(x_1, x_2) R_2(x_1, x_2, x_F), \quad (11)$$

where  $x_i$ ,  $i = 1, 2$ , is the momentum fraction of the  $i^{th}$  quark,  $F_2(x_1, x_2)$  is the two-quark distribution function in the initial hadron and  $R_2(x_1, x_2, x_F)$  is the two-quark recombination function with  $\beta$  a normalization constant which must be fixed by comparison to experimental data. Baryon production can be calculated just by replacing the  $F_2$  and  $R_2$  by the corresponding functions for three quark recombination. Along this work we will use

$$F_i(x_1, \dots, x_i) = \left[ \prod_{j=1}^i f_j(x_j, \mu_F^2) \right] \left( 1 - \sum_{j=1}^i x_j \right)^\gamma$$

$$i = 2, 3, \quad (12)$$

with  $\gamma = 1$  for  $i = 2$  and  $\gamma = -0.1$  for  $i = 3$  [12] and, for the recombination function we shall use its simplest version given by [24, 25]

$$R_i(x_1, \dots, x_i, x_f) = \frac{\prod_{j=1}^i x_j}{x_f^i} \delta \left( 1 - \frac{\sum_{j=1}^i x_j}{x_F} \right) .$$

$$i = 2, 3 \tag{13}$$

## 4 Modeling and comparison to experimental data

Several experiments have measured the differential cross section both as a function of  $x_F$  and  $p_T^2$  for charm meson and also baryon production. A few of them have also measured the production asymmetry, defined by

$$A(x_F) = \frac{dN^L/dx_F - dN^{NL}/dx_F}{dN^L/dx_F + dN^{NL}/dx_F} , \tag{14}$$

where  $L$  is for Leading and  $NL$  is for Non Leading particles.

Along this section we shall compare the production model presented in the preceding section with experimental data for  $D$  meson production in  $\pi^- - Nucleon$  interactions and for  $\Lambda_c$  production in  $\pi, p - Nucleon$  interactions, which are, up to our knowledge, most of the existing data in charm particle production.

In order to compare the theoretical model to experimental data, we will use

$$\frac{d\sigma}{dx_F} = a \frac{d\sigma}{dx_F}^{frag} + b \frac{d\sigma}{dx_F}^{rec} , \tag{15}$$

where the first term in the right hand side of eq. (15) accounts for charm hadron production through fragmentation and its expression is given in eqs. (5), and the second term represents the charm hadron production by the recombination of the perturbatively generated charm quark with spectator quarks, remnants of the beam particles, as given in eq. (6).

We do not include any contribution coming from the direct recombination of the debris of the initial particles (see Sec. 3.3) because it is naturally included when NLO contributions to heavy quark production are taken properly into account, either by including explicitly NLO diagrams in the perturbative part of the process, either through the effective K-factor. However, we recognize that as charm quarks are in the limit of what is understood as a heavy quark, this mechanism is equally good to describe the recombination part of the hadronization process (See e.g. Refs [12, 16, 23]).

Coefficients  $a$  and  $b$  in eq.(15) were fixed by fitting experimental data. In most of the data, the differential cross section for particle and antiparticle production were

fitted independently by minimizing  $\chi^2$  using the model of eq. (15). In these cases we used

$$\chi^2 = \sum_i \left( \frac{y_i - \bar{y}_i}{\sigma_i} \right)^2 \quad (16)$$

to obtain a linear system of equations in the unknowns  $a$  and  $b$  by requiring that  $\chi^2$  has a minimum and then, the resulting  $2 \times 2$  linear system of equations was solved analytically. When fits involved one of the differential cross sections and the asymmetry, the above procedure is not longer possible since a non linear  $4 \times 4$  system of equations is obtained. In these cases we defined a combined  $\chi^2$  as the sum of the  $\chi^2$  for the differential cross section plus the one corresponding to the asymmetry and used MINUIT to perform the fits.

We have to remark that particle and antiparticle  $x_F$  distributions and the production asymmetry form a set of three non-independent measurements. Then we performed fits to two of these measurements and derived the third from the other two.

In the following we analyse charm meson and baryon data and compare with our model in eq. (15).

## 4.1 $D^\pm$ production

Charged  $D$  meson production has been measured in  $\pi^- - Nucleus$  interactions at 350 GeV/ $c$  by the WA92 Experiment [4], 340 GeV/ $c$  by the WA82 Experiment [5], 250 GeV/ $c$  by the E769 Collaboration [6] and 500 GeV/ $c$  by the E791 Collaboration [7]. E769 [8] and E791 [9] Collaborations also measured  $D^{*\pm}$  production in 250 and 500 GeV/ $c$   $\pi^- - Nucleus$  interactions respectively.

In Fig. 6 we display the results of our fit to experimental data on  $D^\pm$  production by the WA92 Collaboration [4]. The WA92 experiment used targets of copper and tungsten. As can be seen in the figures, the model describes quite well the experimental data. Our fit also shows that charm quark fragmentation and recombination of the charm quark produced in the hard QCD process with the debris of the initial beam particles is enough to describe the data. The asymmetry, as shown by the curve in Fig. 6, has been calculated from the curves obtained from fits to particle and antiparticle distributions using eq. (14).

In Fig. 7 we display the results of our fit to experimental data on  $D^\pm$  production and asymmetry by the WA82 Collaboration [5]. Data were obtained using a  $\pi^-$  beam with W/Si and W/Cu targets.

Once again, as evidenced in the figures, the result of the fit describes well the experimental data on both, production and production asymmetry. It has to be noted however that in fits to the  $D^+$  WA82 data, a small contribution from the recombination of the hard QCD charm quark with the debris of the initial pion is necessary, opposite to what happens with the WA92 data. This behavior is due to

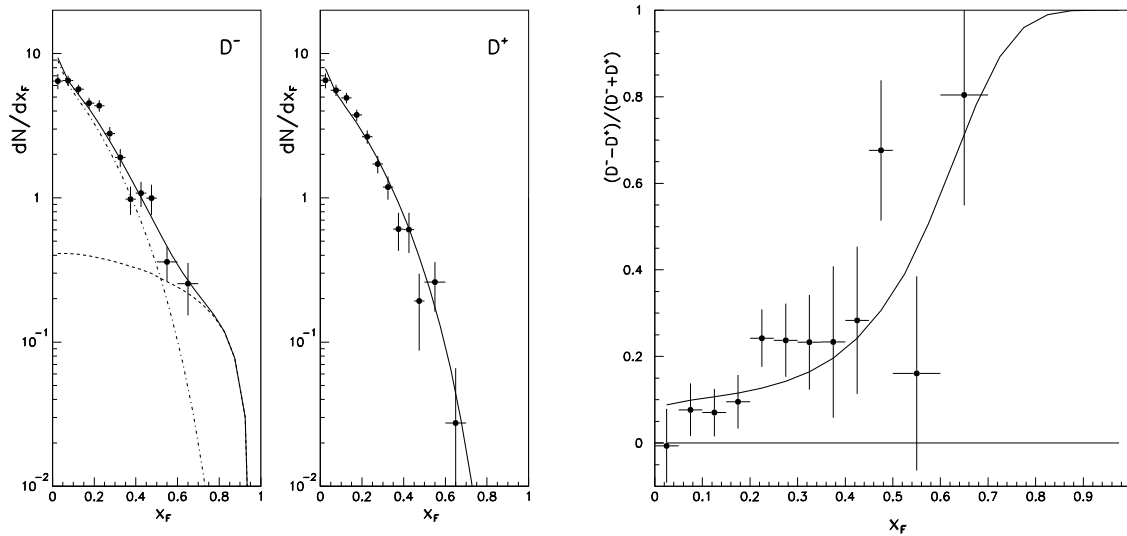


Figure 6:  $D^-$  and  $D^+$  production by the WA92 Collaboration [4]. Left and middle panels: (full line) our model as in eq. (15) compared to experimental data. Dashed and point-dashed lines: contributions from recombination and fragmentation respectively. Right: Production asymmetry. Model (full line) *vs* experimental data.

the high value of the last experimental point, not seen in the WA92  $D^+$  data (See Fig. 6). We also shown in the figure the asymmetry obtained from fits to WA92 [4] and E769 [6] data. As can be seen, both curves are similar and describe well the WA82 data on production asymmetry. Note also that a null contribution from recombination to  $D^+$  production results in an asymmetry growing fast than that shown by the full line in Fig. 7, giving a better agreement among data and model.

In Fig. 8 we show the data and fits to the  $D^*(2010)$  production in 500 GeV/c  $\pi^- Nucleus$  interactions by the E791 Collaboration [9]. The E791 measured the  $D^{*-} + D^{*+}$  particle distribution as a function of  $x_F$  as well as the  $D^{*\pm}$  production asymmetry. In order to fit the data with our model of eq. (15), we fitted simultaneously the  $D^{*-} + D^{*+}$  particle distribution and the production asymmetry. From the fits, we extracted the individual  $D^{*-}$  and  $D^{*+}$  particle distributions. As can be seen in the figure, our curves agree well with the experimental data. Data on  $D^\pm$  production asymmetry from the same experiment [7] is superimposed on the  $D^{*\pm}$  data. As shown in the figure, both charged  $D$  and  $D^*$  asymmetries are the same within errors. The E769 Collaboration has also measured the  $x_F$   $D^{*\pm}$  and  $D^\pm$  distributions and asymmetry in 250 GeV/c  $\pi$ -nucleon interactions [8]. They reported that the behavior of the  $x_F$  particle distributions are of the form  $(1 - x)^{2.9 \pm 0.4}$  and  $(1 - x)^{4.1 \pm 0.5}$  for leading and no-leading  $D^*$  mesons respectively in the region  $0.1 < x_F < 0.6$ . From

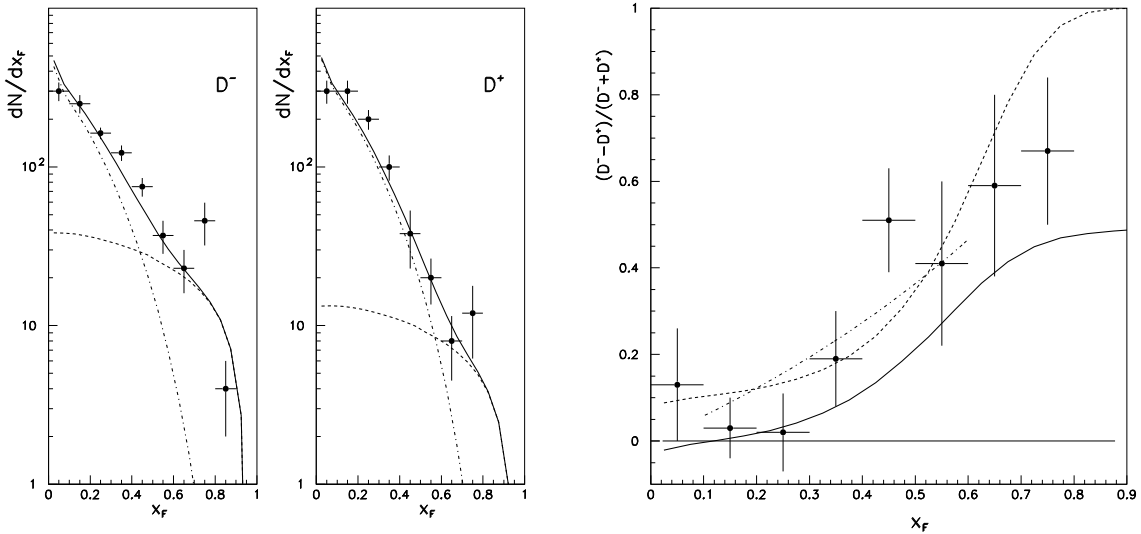


Figure 7: Left:  $D^-$  and  $D^+$  production by the WA82 Collaboration [5]. Left and middle panels: (full line) our model as in eq. (15) compared to experimental data. Dashed and point-dashed lines: contributions from recombination and fragmentation respectively. Right: Production asymmetry. Model (full line) *vs* experimental data. Also shown the asymmetry as fitted to the WA92 data (dashed line) and the one extracted from measurements of the  $D^-$  and  $D^+$   $x_F$  distributions by the E769 Collaboration [6] (dashed-point line).

these fits we extracted the asymmetry shown by the dashed line in Fig. 8, which reproduces the same behavior of our fit to the  $D^{*\pm}$  asymmetry measured by the E791 Collaboration. This gives support to the idea that the production mechanisms of the pseudoscalar  $D^\pm$  and vector  $D^{*\pm}$  mesons are the same, depending only on the flavor content of the initial and final particles.

A comparison of all the data and curves on  $D^\pm$  production asymmetries shows that the asymmetry seems to be independent of the collision energy.

## 4.2 $D^0$ and $\bar{D}^0$ production

In Fig. 9 we display data on  $D^0$  and  $\bar{D}^0$  production by the WA92 [4] experiment and compare to the model of eq. (15). As evidenced in the figure, the model describes quite well the experimental data. Notice that in  $\pi^- - \text{Nucleus}$  interactions, the  $D^0$  ( $c\bar{u}$ ) is leading, then a positive asymmetry is expected. However,  $\bar{u}$  valence quarks of the  $\pi^-$  can annihilate easily with  $u$  valence quarks in the Nucleus, then becoming unavailable to recombine with the charm quark to produce a  $D^0$  state. Consequently

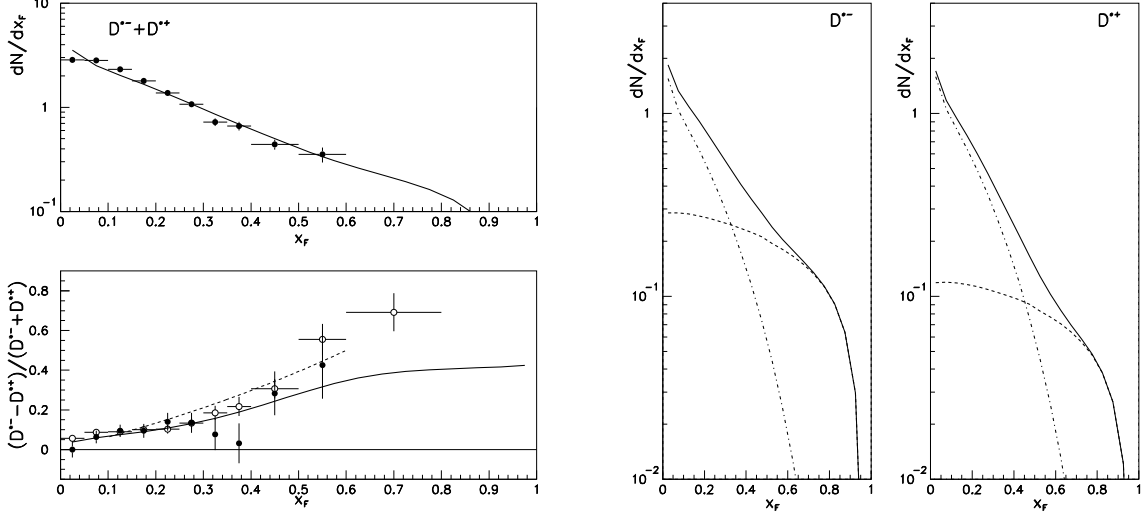


Figure 8: Left:  $D^{*-} + D^{*+}$  production in  $\pi^- Nucleus$  interactions at 500 GeV/c. Data from the E791 Collaboration [9]. Full line: our model as in eq. (15). bottom:  $D^{*-}/D^{*+}$  production asymmetry. Full line: our fit. Data from the E791 Collaboration ( $D^{*-}$ : full circles [9],  $D^{*+}$ : open circles [7]). Right:  $D^{*-}$  and  $D^{*+}$   $x_F$  distributions. Full line:  $dN/dx_F$  as given by eq. (15). Dashed line: contribution from recombination, point-dashed line: fragmentation.

both  $D^0$  and  $\bar{D}^0$  are mainly produced by charm quark fragmentation at the same rate and the asymmetry is largely suppressed as noted in Refs. [12, 26]. Nevertheless, at large  $x_F$  there is an excess of both  $D^0$  and  $\bar{D}^0$  which still requires a small contribution from recombination.

Table 1 lists the results of the fits to experimental data on  $D$  production and asymmetries. As shown in Table 1, the  $\chi^2$  of the fits are in general larger than desirable. This somewhat unpleasant aspect of the fits is mainly due to two reasons, 1) the bad quality of experimental data exhibiting large error bars in most cases and, 2) the small number of parameters of the model, which do not allow to describe the details of the data but the more or less gross features of them.

### 4.3 $\Lambda_c^\pm$ production

In Fig. 10, we display the data and fit results for  $\Lambda_c$  production and production asymmetry obtained in 600 GeV/c  $\pi^- Nucleus$  interactions by the SELEX Collaboration [3]. We display also the E791 [2] data on  $\Lambda_c$  production asymmetry in  $\pi^- - Nucleus$  interactions at 500 GeV/c.

Here we fitted the  $\Lambda_c^+$  and  $\Lambda_c^-$  particle distributions and obtained the asymmetry

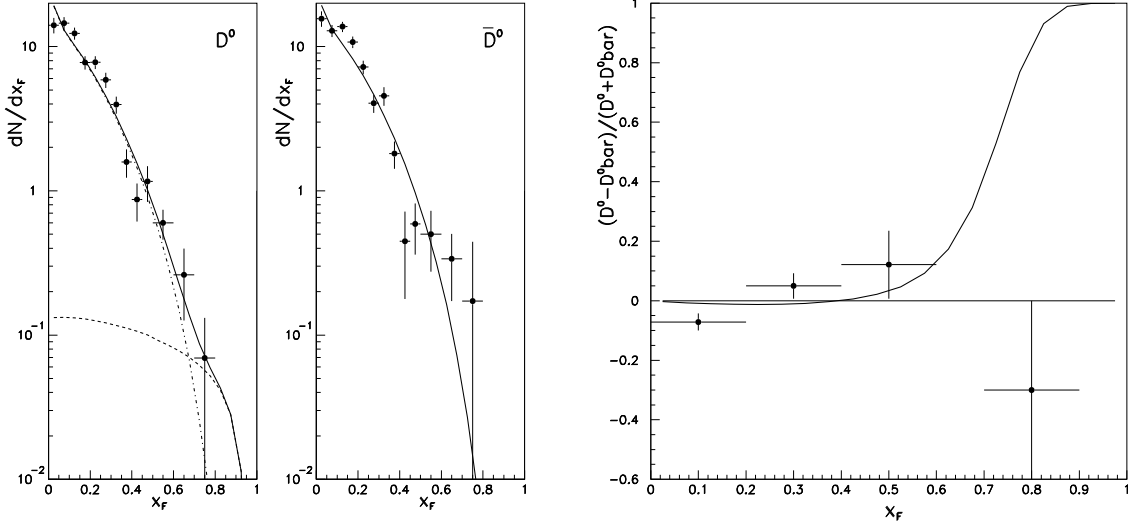


Figure 9:  $D^0$  and  $\bar{D}^0$  production by the WA92 Collaboration [4]. Left and middle panels: (full line) our model as in eq. (15) compared to experimental data. Dashed and point line: contributions from fragmentation and recombination respectively (See the text). Right: Production asymmetry. Model (full line) *vs* experimental data.

from our fitting functions. As can be seen in the figures, our theoretical curves agree well with the experimental data.

It is interesting to note that, although both  $\Lambda_c^+$  ( $udc$ ) and  $\Lambda_c^-$  ( $\bar{u}\bar{d}\bar{c}$ ) are leading in  $\pi^-$  ( $\bar{u}d$ )-Nucleon interactions, there is a significant difference in their  $x_F$  distributions. In fact, as noted in Ref. [16], valence  $\bar{u}$  quarks in the  $\pi^-$  can annihilate easily with (valence)  $u$  quarks in nucleons but, valence  $d$  quarks of the pion cannot, thus favoring the  $\Lambda_c^+$  production over the  $\Lambda_c^-$  one. This is the case of diagrams c) and d) in Fig. 11. However, not only the recombination mechanism contributes to the  $\Lambda_c^\pm$  production asymmetry in  $\pi^-$  Nucleon interactions. Color string fragmentation also gives a contribution. Looking at the diagrams a) and b) in Fig. 11 we note that also in this case  $\Lambda_c^-$  production is disfavored. An analogue diagram to that of Fig. 11 a), with the valence  $d$  quark in the  $\pi^-$  annihilating with a  $\bar{d}$  quark in the proton and a  $\bar{c}$  quark produced in the forward ( $x_F > 0$ ) region giving rise to a  $\Lambda_c^-$  is suppressed by at least two reasons: 1)  $\bar{u}_\pi - u_p$  annihilation is favored over  $d_\pi - \bar{d}_p$  because in the first case both are valence quarks and 2) a  $\bar{c}$  quark produced in the forward region has to form a baryonic color string with a  $\bar{u}\bar{d}$  sea diquark in the proton in order to produce a  $\Lambda_c^-$ . The same situation is present in the case of Fig. 11 d).

Finally, in Fig. 12 we show the data and fits to  $\Lambda_c^\pm$  production and production asymmetry in  $p$   $N$  interactions at 600 GeV/ $c$  [3]. In order to get the theoretical

Experiment	Particle	a	b	$\chi^2/\text{d.o.f.}$
WA82	$D^-$	$14269.27 \pm 1116.82$	$918 \pm 140.57$	3.570
WA82	$D^+$	$18649.11 \pm 1828.77$	$311.99 \pm 128.22$	2.368
WA92	$D^-$	$292.64 \pm 14.59$	$9.59 \pm 2.43$	3.075
WA92	$D^+$	$302.46 \pm 13.92$	$0. \pm 1.34$	1.698
E791	$D^{*-}$	$41.54 \pm 2.14$	$4.86 \pm 0.54$	4.613
E791	$D^{*+}$	$48.40 \pm 2.17$	$1.97 \pm 0.44$	4.613
WA92	$D^0$	$630.74 \pm 29.32$	$4.17 \pm 3.26$	3.137
WA92	$\bar{D}^0$	$733.51 \pm 37.25$	$0. \pm 3.90$	4.370

Table 1: Coefficients obtained in fits to experimental data on  $D$  meson production. The  $\chi^2/\text{d.o.f.}$  of the E791 data on  $D^*$  production is for a simultaneous fit to the  $D^{*-} + D^{*+}$   $x_F$  distribution and asymmetry.

curves, we fitted both the  $\Lambda_c^+$  and  $\Lambda_c^-$  distributions as a function of  $x_F$  and calculated the asymmetry from the curves obtained in fits.

For the  $\Lambda_c^-$  we only use the first term in eq. (15), neglecting any contribution from recombination. The reason is that in order to get a  $\Lambda_c^-$  baryon from recombination, the perturbatively produced  $\bar{c}$  quark has to recombine with a  $\bar{u}\bar{d}$  diquark formed from sea quarks in the initial proton, which is less favorable than the recombination of a  $c$  quark with a  $ud$  valence diquark (see Fig. 13).

As in the case of  $\Lambda_c^\pm$  production in  $\pi^- - \text{Nucleon}$  interactions,  $\Lambda_c^+$  production is favored over the  $\Lambda_c^-$ , having not only a different shape in their  $x_F$  distributions but also a different global normalization, as shown in Fig. 13. This is a distinctive feature of charm baryon production not seen in charm meson production, where both, particle and antiparticle  $x_F$  distributions begin at more or less the same point at  $x_F \sim 0$ .

Concerning the data on the production asymmetry in  $p \text{ Nucleus}$  interactions by SELEX, it is hard to understand, however, how they obtain three points with asymmetry bigger than one. Note that from the definition of the asymmetry follows that it is bounded to be between 1 and  $-1$ .

Table 2 shows the results of fits to experimental data on  $\Lambda_c^\pm$  production. Once again, as in the case of meson production,  $\chi^2$  of fits are far away from their desirable values. However, note that in the case of baryon production, experimental data exhibits larger error bars than in the case of mesons.

## 5 Conclusions

We have shown that using a simple model based on perturbative QCD for charm quark production and on well known hadronization mechanisms, namely fragmenta-



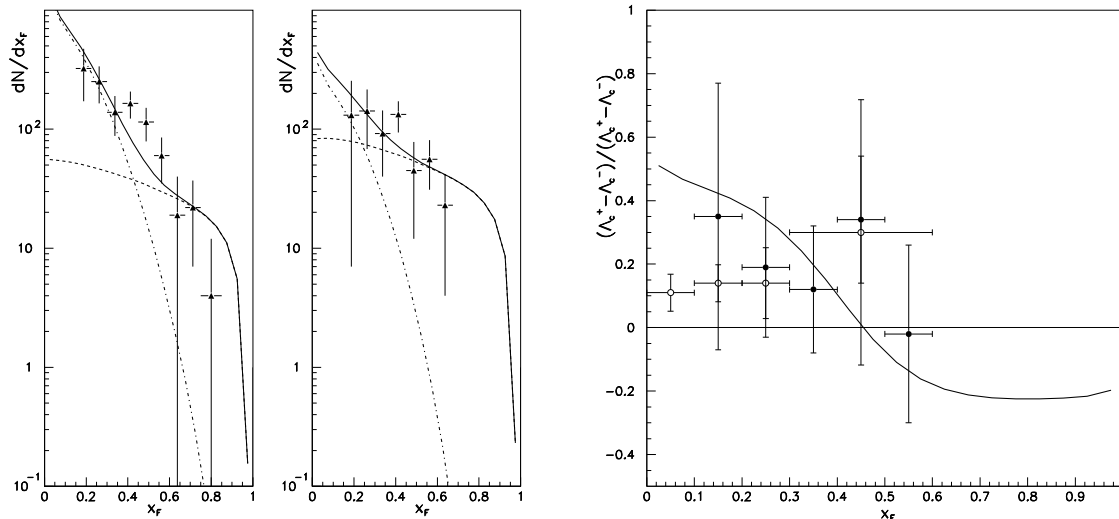


Figure 10:  $\Lambda_c^+$  (left) and  $\Lambda_c^-$  (middle) production in  $\pi^- Nucleus$  interactions at 600 GeV/c. Data from the SELEX Collaboration [3]. Full line: our model as in eq. (15). Right:  $\Lambda_c^+/\Lambda_c^-$  production asymmetry. Data from Ref. [3] (full circles) and Ref. [2] (open circles). Full line: result of our fit.

tion and recombination, the available experimental data on charm hadron production can be well described. The idea of describing charm hadron production by means of fragmentation and recombination of perturbatively produced charm quarks is not new. It has been discussed by the first time in Ref. [10], but never has been extensively tested against most of the available experimental data.

Our analysis shows that intrinsic charm is unnecessary to describe consistently the experimental data on both charm particle  $x_F$  distributions and charm particle production asymmetries. This was evident once SELEX data on  $\Lambda_c$  baryons and antibaryons became available, as noted in Ref. [16].

Parameters in the model of eq. (15) represent the unknowns associated to the relative fractions of the fragmentation and recombination contributions, but also include the uncertainties coming from the non-perturbative contributions to the hadronization process. It is conceivable that with more abundant and precise experimental data, the behavior of this parameters with respect to the reaction and reaction energy can be fixed, allowing in this way a more predictive power of the model.

In Refs. [12, 16] another model including the recombination of charm quarks with the debris of the initial particles was considered. However, in this model, recombining charm quarks were considered as part of the structure of the initial particles. The fact that both, the model discussed here and the model of Refs. [12, 16], are able to

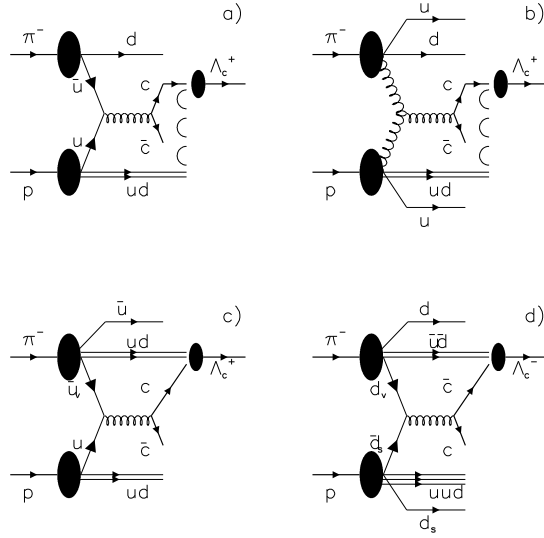


Figure 11: Some typical diagrams for  $\Lambda_c^+$  and  $\Lambda_c^-$  production in  $\pi^- Nucleus$ . a) and b)  $\Lambda_c^+$  production by color string fragmentation. The  $c$  quark forms a baryon-like string with a diquark in the proton. The  $\bar{c}$  quark forms a meson-like string with the remaining valence quark of the  $\pi^-$ . c) and d)  $\Lambda_c^\pm$  production by recombination.

describe well the experimental data is due to the fact that the momentum distribution of perturbatively produced charm quarks is similar to the sea charm quark distribution in hadrons. It is easy to see that this is a consequence of the fact that in both cases the origin of the charm quarks is gluon splitting, then its momentum distributions must be similar.

In addition, we have shown that factorization is broken as long as the structure of the initial colliding particles has to be taken into account in order to describe the hadronization of charm quarks. However, it does not mean that new unknowns are added to the problem. There still exist a consistent way to calculate hadronization within the framework of the recombination model.

Finally, we would like to stress that not only recombination, but also fragmentation, contributes to the observed baryon production asymmetries. In recombination, the asymmetry is a consequence of the sharing of partons among the initial and final particles. In fragmentation, the asymmetry is due to the parton content of the initial particles. Note that, as long as initial particles are baryons and mesons, it is easier to have mesonic and baryonic color string, but no “anti-baryonic” ones, thus baryon production is favored over antibaryon production. This effect does not appear in

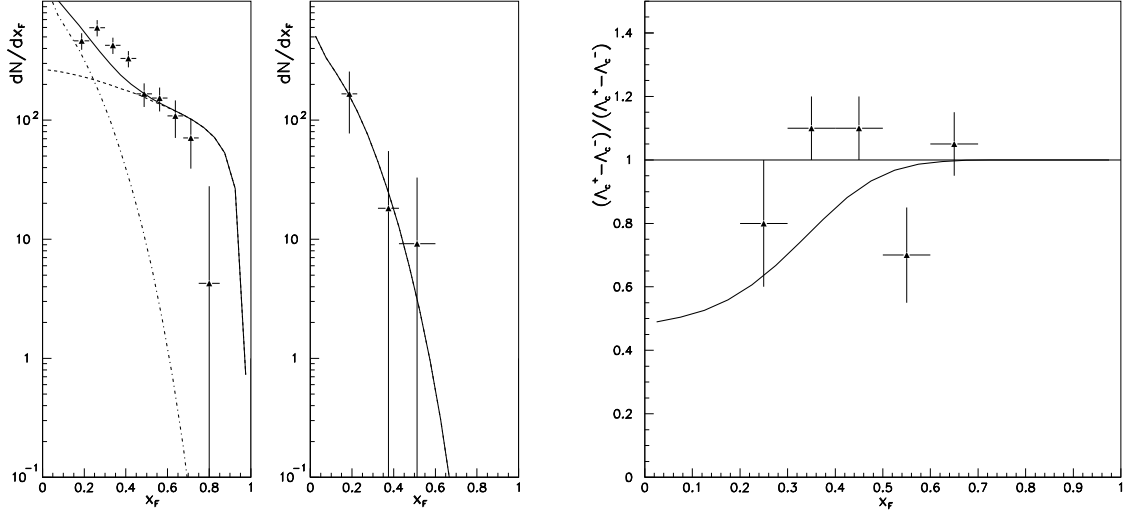


Figure 12:  $\Lambda_c^+$  (left) and  $\Lambda_c^-$  (middle) production in  $p$  *Nucleus* interactions at 600 GeV/c beam energy. Data from the SELEX Collaboration [3]. Full line: our model as in eq. (15). Right:  $\Lambda_c^+/\Lambda_c^-$  production asymmetry. Data from Ref. [3]. Full line: result of our fit.

meson-antimeson production since they are formed mainly from mesonic strings. If antibaryons were used as initial particles, fragmentation would favor the production of antibaryons, producing the opposite effect. It is interesting to note also that recombination gives a small contribution only noticeable at large  $x_F$  (of the order of  $x_F \sim 0.6 - 0.7$ ) to the  $D$  meson  $x_F$  distributions while for baryons its contribution becomes important for  $x_F \sim 0.4$ .

## Acknowledgments

J. Magnin would like to thanks the warm hospitality at the Physics Department, Universidad de los Andes, where part of this work was done. L.M. Mendoza-Navas would like to thanks the warm hospitality at CBPF during his stay for the completion of the work. This works was supported by Fundación para la Promoción de la Investigación y la Tecnología del Banco de la República (Colombia) under contract Project No.: 1376; CNPq, the Brazilian Council for Science and Technology and FAPERJ (Brazil) under contract Project No.: E-26/170.158/2005.

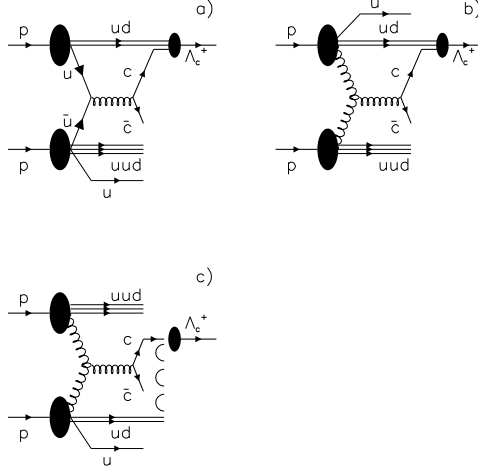


Figure 13: Typical diagrams for  $\Lambda_c^+$  and  $\Lambda_c^-$  production in  $p$  Nucleus. a) and b)  $\Lambda_c^+$  production by recombination. c)  $\Lambda_c^+$  production by color string fragmentation.

Experiment	Particle	a	b	$\chi^2/\text{d.o.f.}$
$\pi^- - N$	$\Lambda_c^+$	$76511.84 \pm 18661.76$	$990.78 \pm 303.93$	1.602
$\pi^- - N$	$\Lambda_c^-$	$22625.39 \pm 18946.02$	$1682.04 \pm 478.72$	0.786
$p - N$	$\Lambda_c^+$	$77904.03 \pm 16361.06$	$5226.22 \pm 608.73$	4.077
$p - N$	$\Lambda_c^+$	$32204.85 \pm 19726.59$	$0.00 \pm 688.32$	0.093

Table 2: Coefficients obtained from fits to data on  $\Lambda_c^\pm$  production from the SELEX Collaboration.

## References

- [1] P. Nason, S. Dawson and R.K. Ellis, Nucl. Phys. **B 327** (1989) 49.
- [2] E.M. Aitala *et al.* (E791 Collaboration), Phys. Lett. **B 495** (2000) 42.
- [3] F.G. Garcia *et al.* (SELEX Collaboration), Phys. Lett. **B 528** (2002) 49.
- [4] M. Adamovich *et al.* (WA92 Collaboration), Nucl Phys. **B495** (1997) 3.
- [5] M. Adamovich *et al.* (WA82 Collaboration), Phys. Lett. **B305** (1993) 402.
- [6] G.A. Alves *et al.* (E769 Collaboration), Phys. Rev. Lett. **69** (1992) 3147.

- [7] E.M. Aitala *et al.* (E791 Collaboration), Phys. Lett. **B371** (1996) 157.
- [8] G.A. Alves *et al.* (E769 Collaboration), Phys. Rev **D49** (1994) R4317; *ibid.* Phys. Rev. Lett. **72** (1994) 812.
- [9] E.M. Aitala *et al.* (E791 Collaboration), Phys. Lett. **B539** (2002) 218.
- [10] V.G. Kartvelishvili, A.K. Likhoded and S.R. Slabospitskii, Sov. J. Nucl. Phys. **28** (1978) 678; *ibid.* **33** (1981) 434.
- [11] S.J. Brodsky, P. Hoyer, C. Peterson and N. Sakai, Phys. Lett. **B 93** (1980) 451; S.J. Brodsky, C. Peterson and N. Sakai, Phys. Rev. **D 23** (1981) 2745.
- [12] E. Cuautle, G. Herrera and J. Magnin, Eur. Phys. J. **C 2** (1998) 473; G. Herrera and J. Magnin, Eur. Phys. J. **C 2** (1998) 477; J. dos Anjos, G. Herrera, J. Magnin and F.R.A. Simão, Phys. Rev. **D 56** (1997) 394.
- [13] O.I. Piskunova, Phys. Atom. Nucl. **66** (2003) 307 and references therein.
- [14] E. Braten, M. Kusunoki, Yu Jia and T. Mehen, Phys. Rev. **D70** (2004) 054021; E. Braten, Yu Jia and T. Mehen, Phys. Rev. Lett. **89** (2002) 122002.
- [15] R. Rapp and E.V. Shuryak, Phys. Rev. **D67** (2003) 074036.
- [16] J.C. Anjos, J. Magnin and G. Herrera, Phys. Lett. **B 523** (2001) 29.
- [17] J. Babcock, D. Sivers and S. Wolfram, Phys. Rev. **D 18** (1978) 162; R.K. Ellis, Fermilab-Conf-89/168-T (1989); I. Inchliffe, Lectures at the 1989 SLAC Summer Institute, LBL-28468 (1989).
- [18] B.L. Combridge, Nucl. Phys. **B 151** (1979) 429.
- [19] S. Frixione, M.L. Mangano, P. Nason and G. Ridolfi, Nucl. Phys. **B431** (1994) 453.
- [20] C. Peterson, D. Schlatter, J. Schmitt and P. Zerwas, Phys. Rev. **D 27** (1983) 105.
- [21] G.H. Arakelian, A. Capella, A.B. Kaidalov, Yu.M.Shabelski, hep-ph/0103337; K. Boreskov, A. Capella, A. Kaidalov, J. Tran Thana Van, Phys. Rev. **D47** (1993) 919.
- [22] **Review of Particle Physics**, K. Hagiwara *et al.*, Phys. Rev. **D66** (2002), pag. 138.

- [23] J. Magnin and L.M. Mendoza-Navas, hep-ph/0009198, also in Proceedings of the 3rd Latin American Symposium on High Energy Physics. Ed. E. Nardi, JHEP-Proceedings (2000).
- [24] K.P. Das and R.C. Hwa, Phys. Lett. **B68** (1977) 459; Erratum *ibid.* **B73** (1978) 504.
- [25] J. Ranft, Phys. Rev. **D 18** (1978) 1491.
- [26] V.A. Bednyakov, Mod. Phys. Lett. **A10** (1995) 61.